EUROPEAN FUSION DEVELOPMENT AGREEMENT

EFDA–JET–CP(07)02-02

D. Moreau, D. Mazon, M. Ariola, G. De Tommasi, A. Boboc, M. Brix, J. Brzozowski, V. Cocilovo, R. Felton, N. Hawkes, R. King, L. Laborde, T. Loarer, E.de la Luna, I. Nunes, F. Piccolo, F. Sartori, E. Surrey, L. Zabeo, O. Zimmerman and JET EFDA contributors

Real-Time Profile Control for Advanced Tokamak Operation on JET

Real-Time Profile Control for Advanced Tokamak Operation on JET

D. Moreau[1], D. Mazon[1], M. Ariola[2], G. De Tommasi[2], A. Boboc[3], M. Brix[3], J. Brzozowski[4], V. Cocilovo[5], R. Felton[3], N. Hawkes[3], R. King[3], L. Laborde[3], T. Loarer[1], E.de la Luna[6], I. Nunes[7], F. Piccolo[3], F. Sartori[3], E. Surrey[3], L. Zabeo[3], O. Zimmerman[8]
and JET EFDA contributors*

[1]EURATOM-CEA Association, DSM-DRFC, Cadarache, 13108, St Paul lez Durance, France
[2]EURATOM-ENEA-CREATE Association, Univ. Napoli Federico II, I-80125 Napoli, Italy
[3]EURATOM-UKAEA Association, Culham Science Centre, Abingdon, OX14 3DB, U.K.
[4]EURATOM-VR Association, Fusion Plasma Physics, EES, KTH, Sweden
[5]EURATOM-ENEA Association, C.R. Frascati, 00044 Frascati, Italy
[6]Laboratorio Nacional de Fusion, Asociacion EURATOM-CIEMAT, Madrid, Spain
[7]Centro de Fusao Nuclear, Associaçao EURATOM-IST, Lisboa, Portugal
[8]Institut für Plasmaphysik, Forschungszentrum J¸lich GmbH, Association FZJ-EURATOM,
** See annex of M.L. Watkins et al, "Overview of JET Results ",*
(Proc. 21st IAEA Fusion Energy Conference, Chengdu, China (2006)).

Preprint of Paper to be submitted for publication in Proceedings of the
5th IAEA TM on Steady State Operation of Magnetic Fusion Devices,
(Daejeon, Republic of Korea 14th - 17th May 2007)

ABSTRACT.

Real-time simultaneous control of several radially distributed magnetic and kinetic plasma parameters (such as the safety factor, q(x), and gyro-normalized temperature gradient, ρ_{Te}*(x), respectively) is being investigated on JET, in view of developing integrated control of advanced tokamak scenarios and internal transport barriers suitable for ITER. This paper describes the new model-based optimal profile controller which has been tested during the last experimental campaign. The controller aims to use the combination of heating and current drive systems - and optionally the Poloidal Field (PF) system - in an optimal way to regulate the evolution of several parameters. In the first part of the paper, a technique for the experimental identification of a dynamic plasma model is described, taking into account the physical structure and couplings of the transport equations, but making no quantitative assumptions on the transport coefficients or on their dependences. To cope with the high dimensionality of the state space and the large ratio between the various time scales involved, the model identification procedure and controller design both make use of the theory of singularly perturbed systems by means of a multiple-time-scale approximation. The second part of the paper deals with the control theory and algorithm. Conventional optimal control is recovered in the limiting case where the ratio of the plasma confinement time to the resistive diffusion time vanishes. Closed-loop simulations of the new controller have been performed in preparation for experiments, and some results are shown. Finally, in the last part of the paper, first experimental results of current profile control obtained during the last 2007 JET campaign are presented and discussed.

1. INTRODUCTION

During the 2002-2004 experimental campaigns on JET, real-time control of radially distributed parameters, such as the current and electron temperature gradient profiles, was achieved for the first time [1-3]. This was the initial step of an ongoing long-term research program which aims to ultimately develop integrated control of steady state advanced tokamak scenarios and Internal Transport Barriers (ITB) in ITER. At this stage, and for the sake of simplicity, the controller was based on the static plasma response only and on an algorithm that minimises a weighted sum of least square integral errors between requested magnetic and kinetic profiles (known to be strongly coupled) and measured ones [4]. Such an integrated strategy is particularly relevant to future fusion devices such as ITER where the Heating and Current Drive (H&CD) actuator systems will not be very flexible. It will be essential when more controls need to be included into the scheme to regulate the fusion burn.

Another characteristic of the profile control investigations on JET is the use of the available actuators in their routine operating mode, i.e. avoiding features that may not extrapolate to burning plasmas. In ITER, some actuators may be less versatile than in present-day tokamaks, due to simple physics and/or technology considerations (antenna design, wave propagation, etc..). An example can be found at JET: controlling accurately the radial deposition of Lower Hybrid (LH) waves through the launched n// spectrum [5-6] could be introduced within the proposed JET distributed-

parameter control algorithm [4], but it does not appear practical in high-beta fusion plasmas and was therefore not implemented. Another point can be discussed: tailoring in ITER the off-axis non-inductive current density through a unique actuator dedicated to this task (e.g. by dedicated Neutral Beams (NB), or by additional Electron Cyclotron (EC) or LH waves as is usually done) will be become more difficult in the presence of a large bootstrap current and of alpha-particle heating.

The approach newly developed at JET aims to use the combination of H&CD/PF (poloidal field) systems and the experimentally deduced plasma couplings in the most efficient dynamic way to achieve a set of simultaneous tasks. In this respect, it stands in contrast with experiments in which a one-to-one correspondence between a given actuator and a scalar output characterising a plasma profile is assumed (e.g. LH power and internal inductance) The experiments using the static plasma response controller were successful in achieving the various targets that were aimed at, thus demonstrating the validity of the coupled profiles approach [4]. However, it was found to be too sensitive to rapid plasma events such as the spontaneous emergence of transient ITBs or MHD instabilities. In order to address this issue, a technique for the experimental identification of a dynamic plasma model has been developed, taking into account the physical structure and couplings of the transport equations, but making no quantitative assumptions on the transport coefficients or on their dependences. The next section describes the theoretical analysis which leads to the choice of the relevant state variables, and the physical constraints to be imposed on the corresponding state-space model. The high dimensionality of the state space and the large ratio between the various time scales involved (resistive and thermal diffusions with strong interactions between fast and slow dynamic modes) call for an appropriate model identification procedure. The technique makes use of a multiple-time-scale approximation and of the theory of singularly perturbed systems. It generates a slow and a fast model of reduced orders which are shown to describe the system satisfactorily.

The third section of the paper concerns the theory leading to the controller design. The control is near-optimal in the sense that it asymptotically merges into conventional optimal control in the limiting case where ε (the ratio of the fast and slow timescales) vanishes. The paper then describes closed-loop simulations in which the radial profiles of the plasma safety factor and of the gyro-normalized electron temperature gradient [7] are controlled simultaneously. The fourth part of the paper finally presents some recent preliminary application of this new controller to the control of the current density profile.

2. IDENTIFICATION OF A STATE-SPACE PLASMA RESPONSE MODEL

2.1. STRUCTURE OF THE DYNAMIC PLASMA MODEL AND PHYSICALLY RELEVANT STATE VARIABLES

In order to use optimal control theory and regulate the plasma evolution in advanced tokamak scenarios, a physics-based technique has been developed to experimentally identify a dynamic, one-fluid plasma model valid in some broad vicinity of an equilibrium state. The structure of the

model stems from a set of transport equations,

$$\mu_0 \frac{\partial j}{\partial t} = -\nabla \times \nabla \times E, \qquad \frac{\partial n}{\partial t} = -\nabla.\Gamma + S_n, \qquad \frac{3}{2}\frac{\partial (nT)}{\partial t} = -\nabla.Q + S_T \tag{1}$$

in which couplings are retained with no loss of generality. The system (Eq. 1) is linearized around an equilibrium reference state (which need not be known explicitly) so that it can ultimately be cast in the generic form of a state space model, a form commonly used in control engineering. In doing so, the state variables appear naturally to be the variations of the internal poloidal magnetic flux, Ψ, and of the temperature, T, and the state space model reads:

$$\partial\Psi/\partial t = A_{11}\Psi(t)+A_{12}\ T(t)+B_{11}\,P(t)+B_{12}\ n(t)+U.V+B_{ext} \tag{2a}$$

$$\varepsilon\partial T/\partial t = A_{21}\Psi(t)+A_{22}\ T(t)+B_{21}\,P(t)+B_{22}\ n(t) \tag{2b}$$

with inputs $P = [P_{LH}, P_{NBI}, P_{ICRH}]$, the heating and current drive input powers, and V_{ext}, the surface loop voltage. The distributed variables $\Psi(x)$ and T(x), where x is a radial coordinate, are projected onto a finite set of trial functions (cubic splines, see Fig.1a) using a Galerkin scheme so that the original partial differential system of equations reduces to an ordinary linear differential system where U is known and $A_{i,j}$, $B_{i,j}$ are matrices of appropriate dimensions which are to be identified from experimental data.

The small (constant) parameter, ε, represents the ratio between the energy confinement time and the characteristic resistive diffusion time ($\varepsilon<<1$), and is introduced here to scale matrices A and B so that their coefficients have similar magnitudes. In the JET experiments, the density profile is not controlled in real time for the moment, so the variations of the plasma density, n, will be considered as disturbances (n is treated as an additional system input but not as an actuator). The main assumptions leading to (Eq.2) are enumerated in Ref. [8].

2.2. TWO-TIME-SCALE APPROXIMATION AND CONTROLLED OUTPUT PARAMETERS

Even when using computer simulated data, the identification of a full-order model (Eq.1-2) proves very difficult (ill-conditionned). This is partly due to the various time scales involved, hence, no attempt has been made using noisy experimental data. To take advantage of the small parameter ($\varepsilon \approx 0.05$ in JET), and noting that ε is going to be even smaller in a burning plasma, the control technique proposed here is based upon the theory of singularly perturbed systems and multiple-time-scale expansions [9]. We therefore seek two models of reduced orders, a slow model,

$$\partial\Psi/\partial t = A_s\Psi+B_s u_s \quad \text{together with} \quad T_s C_s\Psi+D_s u_s \tag{3}$$

and a fast model ($\tau = t / \varepsilon$),

$$\partial T_f / \partial \tau = A_f T_f + B_f u_f \tag{4}$$

where $T=T_s+T_f$, and where u_s and u_f are the slow and fast components, respectively, of a vector, $u=u_s+u_f$, containing all the inputs (P, n and V_{ext}).

Having identified a set of relevant state variables, it can prove practical to apply the control to some output parameters which are more directly linked with MHD stability or ITB physics, and, if possible, are non-dimensional variables so that the range of their optimum target values is known and does not depend on the engineering parameters (magnetic field, current, shape, etc...) of a particular plasma discharge. The safety factor, q(x), and gyro-normalized temperature gradient, ρ_{Te}*(x), have been chosen [1-4] and are thus introduced into the state-space model (to make use of some obvious linearity between the current density and the poloidal flux, the inverse of the safety factor, ι ((x)) = 1/q(x), is used to describe the current density profile). As for Ψ((x)) and T ((x)), a Galerkin approximation is used and in the following, the notations Ψ, T, μ and ρ will refer to the coefficients of the Ψ (x)), T ((x)), ι ((x)) and ρ_{Te}*(x) expansions, respectively. The same cubic splines are used for ι ((x)), Ψ ((x)) and T ((x)) (Fig.1a), but a piecewise linear fit was shown to be a better choice for ρ_{Te}*(x)) (with basis functions shown on Fig.1b) as it involves the gradient of a noisy signal and requires a stronger smoothing [2]. Noticing that ι ((x)) ∝ ∇Y ((x)) and ρ_{Te}* ((x)) ∝ ∇Te ((x))/√Te(x)), linearizing these expressions, differentiating the basis functions and assuming that the time variations of factors such as the toroidal magnetic field and toroidal magnetic flux are not essential and do not depend intrinsically on the power inputs, it appears relevant to seek a model with direct matrix relations between the Galerkin coefficients Ψ and μ, on one hand, and between T and ρ on the other hand. Within the two-time-scale approximation, this yields:

$$= C_{,\psi}.\Psi \quad \text{and} \quad \rho_s = C_{\rho,\psi}\Psi + D_{\rho,\psi}u_s \qquad (\text{or} \quad \rho_s = C_{\rho,} \quad + D_{\rho,} \; u_s) \tag{5}$$

and

$$\rho_f = C_{\rho,T}.T_f \tag{6}$$

which complete the system (Eq. 3-4). It follows that state-feedback control can be applied directly to the variables [μ, ρ] rather than a less robust output-feedback control for which the closed-loop stability of the high-frequency dynamics would not be guaranteed [9].

2.3. PRACTICAL MODEL IDENTIFICATION

A series of interactive routines have been developed to numerically identify the various elements of two-time-scale state-space plasma models, either from experimental data as shown below or, as in Ref. [8], from data obtained through semi-empirical time-dependent simulations of the plasma evolution with large transport codes. It would indeed be more satisfactory to use the latter procedure and design the controller prior to running any real experiment. However, using the JETTO code to

simulate previous control experiments based only on the static plasma response, it was found that the resulting controller gain matrices were significantly different from the experimentally deduced ones [10]. A fortiori, the present understanding of plasma transport phenomena is thought to be insufficient to make reliable predictions of the dynamic response of the plasma, especially in the advanced operation scenarios. Hence, for the time being, dedicated open-loop experiments are necessary to collect the required data before running the model identification codes. The codes rely heavily on system identification algorithms described in [11] and on the corresponding MATLAB' Identification Toolbox functions. They run on the JET cluster of UNIX workstations.

The linearization which is at the origin of the state-space model assumes that all data (inputs, outputs and state variables) are defined with respect to a reference equilibrium state which corresponds to a given set of plasma parameters and input powers (Fig.2). In the advanced scenarios case, JET pulses are generally too short to reach a well-defined equilibrium state so that such a state cannot be determined accurately, but some data processing allows the approximate model matrices to be found without explicit knowledge of the reference state. This is shown on Fig.3 where the free-dynamics of the Ψ Galerkin coefficients obtained from the model for the splines which are maximum at knots 0.4, 0.5 and 0.6 are compared with the corresponding experimental data. The eigenvalues of A_s correspond to time constants of 5.2s, 1.7s and 0.4s.

In a second step, B_s was identified using a pulse with slow modulations of the inputs (Fig.2) while fixing A_s as found above, and a comparison between the model response and the experimental data is shown on Fig.4. The rest of the slow model (Eq.5-6) does not involve time derivatives, and the associated matrices ($C_{\mu,\psi}$, $C_{\rho,\mu}$, $D_{\rho,\mu}$, ...) have been determined via a "least square division" of the relevant time-dependent data. By construction, this simple operation provides a fairly good fit to the data in the domain where the linearization applies.

The fast model identification relies on experiments in which input powers must be modulated at high frequency (20-100Hz), and that forces A_f and B_f to be identified simultaneously. However, noting from Eq. (2b), (3) and (4) that $D_s = -A_f^{-1}.B_f$, one is able to limit the number of matrix elements to identify. To illustrate the method, results are displayed on Fig.5 for 3 Galerkin coefficients of the T_e profile corresponding to the splines which are maximum at the same knots as previously for Ψ. Finally, $C_{\rho,T}$ was found via a "least square division" of the relevant fast data.

3. PROFILE CONTROLLER DESIGN AND CLOSED-LOOP SIMULATIONS

The two-time-scale controller is organized around two main loops [9]:

(i) a slow, proportional-Plus-Integral (PI), regulator control loop which drives the system towards a prescribed equilibrium target state on a resistive diffusion time scale on the basis of the reduced-order slow model, and regulates its evolution. The slow variation of the kinetic variables on the same time-scale is governed by the evolution of the magnetic variables and by the slow feedback evolution of the H&CD actuator powers ;

(ii) a fast proportional control loop which ensures the stability of the kinetic variables on the

plasma confinement time scale, maintaining them on an evolving thermal equilibrium which, at any time, is consistent with the magnetic configuration. This loop regulates their transient behaviour when they are subject to rapid disturbances along the slow trajectory.

The generic behaviour of the system can be schematically described using the diagram displayed on Fig.6. In addition, the present Profile Controller (PC) has been designed to run in two operational modes:

(i) the total plasma current can either be separately controlled together with the plasma shape through the PF system (normal use of the JET Extreme Shape Controller [12]),

(ii) or more loosely by the PC (q-profile control) while the PF system controls the plasma shape *and* the boundary flux. In the latter case, the PC provides the external magnetic flux request, and part of the PF system is used as an additional PC actuator.

3.1. NEAR-OPTIMAL CONTROL: THE SLOW PI LOOP AND THE FAST LOOP

Given a slow and a fast dynamical system under the form of Eq. (3-6), with a state variable $X=X_s+X_f$, and under a set of reasonable controllability conditions [9], the theory of linear-quadratic optimal control and of singularly perturbed systems can be used to find a slow control law, $u_s(t)=-G_s.X_s(t)$ and a fast one, $u_f(t)=-G_f.X_f(t)$, so that $u(t)=u_s(t)+u_f(t)$ minimizes the cost functional (here all variables are reduced by their target values):

$$J\,[u(t)] = \int_0^{\infty} X^{+}(t)\, Q\, X(t)\, dt + \int_0^{\infty} u^{+}(t) R\, u(t)\, dt \qquad (7)$$

where Q and R are positive-definite matrices that allow a compromise between the controller performance and the cost in terms of actuator power. The optimal gains, G_s and G_f, can be found from the solutions of two Riccati equations and ensure the stability of the closed-loop system. Conventional optimal control is recovered when the ratio of the thermal confinement time to the resistive diffusion time vanishes so that the small ε approximate model holds true.

Because of the infinite dimensionality of the system and the limited number of actuators, the controller cannot achieve any possible final state. Given a set of target profiles $[\iota_{target}(x), \rho^{*}_{Te,target}(x)]$, we define the best achievable state with the available actuators as the one which minimizes the quadratic functional (λ_{ITB} is a chosen weighting parameter):

$$I = \int_{x1}^{x2} \left[\iota(x) - \iota_{target}(x)\right]^2 dx + \lambda_{ITB} \int_{x3}^{x4} \left[\rho^{*}_{Te}(x) - \rho^{*}_{Te target}(x)\right]^2 dx \qquad (8)$$

Now, in order to ensure that the best achievable state is reached with no steady state offset, a time integral of the error signals can be included in the slow control law. This is achieved by considering X_s as the union of the slow controlled variables, $[\mu, \rho_s]$, and of a set of linear combinations of their time integrals, of the size of the input vector. The slow PI control law then reads $u_s(t) = -\{G_{sp}.\mu(t)+G_{si}.H.\bullet+d\tau\,[\mu(t), \rho_s(\tau)]\}$. By appropriately linking the matrices Q and H with the basis

functions, it can be shown that in the static limit, I is minimum.

By definition, the high frequency components of all the kinetic variables vanish when the system reaches steady state. They are however subject to perturbations or could even become unstable at some point. The fast proportional control law, $u_f(t) = -G_f.\rho_f(t)$, is to regulate/stabilize the fast variables, $\rho_f(t) = \rho(t) - \rho_s(t)$, where ρ_s is estimated through Eq. (5).

3.2. CLOSED-LOOP SIMULATIONS AND RESULTS

As an illustration of the possible controller performance and time response, we display here typical results of closed-loop simulations performed with the SIMULINK' software. These simulations have been performed assuming that the plasma response is governed by a full-order state space model which, in the limit $\varepsilon \rightarrow 0$, reproduces the reduced-order models which were described in section 2.3 (see Fig.2-5).

Figure 7 shows the rapid initial jump of the kinetic variables towards their slow trajectories ($\rho_f \approx 0$) within a characteristic time of about 0.3s. This is followed by the slow evolution of both magnetic and kinetic variables towards the requested targets which are reached in approximately 4-5s. The effect of a feedforward compensation of known disturbances such as density perturbations (which can have both a physical impact on the profile evolution and a non-physical systematic influence on the q-profile reconstruction) is also shown. A 25% density perturbation has been applied at t = 5s. Figures 7 and 9 show that the excursion of the controlled parameters at the onset of the density perturbation is reduced when the feedforward disturbance rejection scheme is added to the feedback controller.

4. FIRST EXPERIMENTAL RESULTS

The next step was naturally to apply this controller to a real plasma discharge. In order to validate the controller. As a first step, we concentrated during the 2007 campaign on the control of the q-profile only. The main actuators were LH, ICRH, NBI powers and the loop voltage. Following the strategy described in section 2.4, preliminary open-loop experiments were performed with modulations of these actuators around a reference steady state in order to identify the plasma model. The chosen scenario for performing both open and closed-loop experiments was at high triangularity ($\delta = 0.45$) with a toroidal field of 3T, a plasma current of 1.5MA, and an average density of about $3.5.10^{19}\ m^{-3}$. Examples of such modulations of the heating and current drive actuators are given in Fig.10 and Fig.11. Since the q-profile evolves on the resistive time scale, these modulations were done at low frequencies. In the same way, control of the boundary flux was made available (see Fig.12a,b) thanks to the progress realised by the JET Extreme Shape Controller project [12]. Comparison between the iota data reconstructed in real-time (ten iota values at regularly spaced normalised radii) and the simulated data using the identified model can be seen in Fig.13-14-15. The model is found to be sufficiently accurate either when only one actuator like NBI power or Vloop is modulated (Figures 13 and 14, respectively) or when several actuators are modulated simultaneously (Fig.15).

Then, feedback control experiments of the current profile were performed. First of all, in order to test the use of the boundary flux in the PC controller, a single-input single-output control was performed. It consists of the control of the q_{edge} value using the loop voltage as the only actuator. Evidence of such control is shown in Fig.16 where time evolutions of q_{edge} for 2 similar discharges is presented as well as the request on the loop voltage in Fig.17 as calculated by the PC. Note that the chosen target is effectively reached with good reproducibility. This control was performed during the main heating phase, when the plasma current is in general maintained constant. A similar experiment was performed during the current ramp up (see Figures 8-19), and despite the fact that the model is linear and was identified in the vicinity of the current flat top, the controller reaches again the target. The plasma current is raised from 1.2MA up to 1.8MA in less than 1s in order to reach the requested q_{edge} target. This can be generalized to preform part or all of the q-profile during current ramp up, using additional actuators (e.g. LHCD).

All these examples showed the same behaviour when the feedback starts, namely an oscillatory transient in the delivered boundary flux, by which the loop voltage strongly departs from the requested one (Fig.17), thus delaying the time when the control is effective and the target is reached.

Finally, control of the q-profile was performed during more than 7s, using the 3 H&CD systems while requesting the loop voltage to be constant (see Figures 20&21), and was then attempted using 4 actuators including the loop voltage (Fig.22). An important step has been made, validating the proposed integrated control methodology for controlling the q profile, although some improvements are needed for a practical use of the ohmic drive (PF system) as an additional actuator.

CONCLUSION

A system identification procedure has been developed and applied to JET experimental data in order to possibly regulate the dynamics of advanced scenarios through model-based optimal profile control. A technique using singular perturbation methods and a two-time-scale approximation can cope with the high dimensionality of the system and the small ratio between the confinement and resistive diffusion time scales, and yield satisfactory results. A controller based on the same approximation has been designed. It uses a near-optimal control algorithm which amounts to conventional optimal control when the ratio of the two time scales vanishes. Simulations show that magnetic and kinetic profiles can be regulated, at least in the vicinity of a given reference state where the model applies. Further closed-loop experiments are required to assess whether the response models are accurate enough for the radial profiles of the safety factor, q(x), and gyro-normalized electron temperature gradient, $\rho_{Te}^*(x)$, to be simultaneously controlled in real-time. Using the H&CD systems together with the PF system for controlling *(i)* the plasma shape, *(ii)* the magnetic and kinetic plasma profiles (ITB), and *(iii)* the boundary flux, would then provide the essential part of an integrated scheme for ultimately achieving non-inductively driven advanced tokamak discharges in JET and possibly in ITER.

REFERENCES

[1]. MOREAU, D., et al., “Development of Integrated Real-Time Control of Internal Transport Barriers in Advanced Operation Scenarios on JET”, Fusion Energy 2004 (Proc. 20th Int. Conf. Vilamoura, 2004), IAEA-CSP-25/CD, IAEA, Vienna (2005), CD-ROM file EX_P2_5, http://www-naweb.iaea.org/programmes/napc/physics/fec/fec2004/datasets/EX_P2-5.html.

[2]. LABORDE, L., et al., “A Model-Based Technique for Integrated Real-Time Profile Control in the JET Tokamak”, Plasma Phys. Contr. Fus. **47** (2005) 155.

[3]. MAZON, D., et al., “Active Control of the Current Density Profile in JET”, Plasma Phys. Contr. Fus. **45** (2003) L47.

[4]. MOREAU, D., et al., “Real-Time Control of the q-Profile in JET for Steady State Advanced Tokamak Operation”, Nucl. Fusion **43** (2003) 870.

[5]. SUZUKI, T., et al., “Steady State High betaN Discharges and Real-Time Control of Current Profile in JT-60U”, Fusion Energy 2004 (Proc. 20th Int. Conf. Vilamoura, 2004), IAEA-CSP-25/CD, IAEA, Vienna (2005), CD-ROM file EX_1_3, http://www-naweb.iaea.org/programmes/napc/physics/fec/fec2004/datasets/EX_1-3.html.

[6]. MAZON, D., et al., “New Real-Time Profile Controls for Steady State Operation in Tore Supra”, Proc. 33rd EPS Conf. on Plasma Physics, Roma (2006), paper O3.018.

[7]. TRESSET, G., et al., “A Dimensionless Criterion for Characterising Internal Transport Barriers in JET”, Nucl. Fusion **42** (2002) 520.

[8]. MOREAU, D., et al., “Identification of the Dynamic Plasma Response for Integrated Profile Control in Advanced Scenarios on JET”, Proc. 33rd EPS Conf. on Plasma Physics, Roma (2006), paper P1.069.

[9]. KOKOTOVITCH, P.V., KHALIL, H.K., O’REILLY, J., Singular Perturbation Methods in Control: Analysis and Design, Academic Press, London (1986).

[10]. TALA, T., et al., “Predictive Transport Simulations of Real-Time Profile Control in JET Advanced Tokamak Plasmas”, Nucl. Fusion **45** (2005) 1027.

[11]. LJUNG, L., System Identification: Theory for the User, Prenctice Hall PTR (1999).

[12]. AMBROSINO, G., et al., “A New Shape Controller for Extremely Shaped Plasmas in JET”, Fusion Engineering and Design **66-68** (2003) 797.

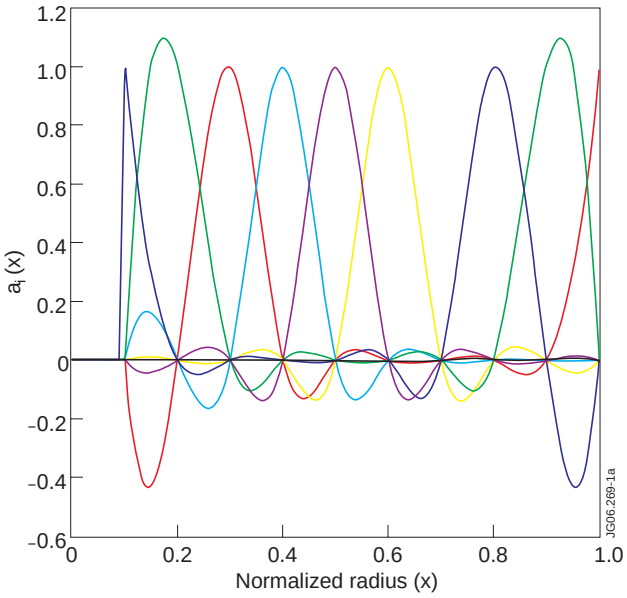

Figure 1a. Cubic splines used for Ψ, ι and T.

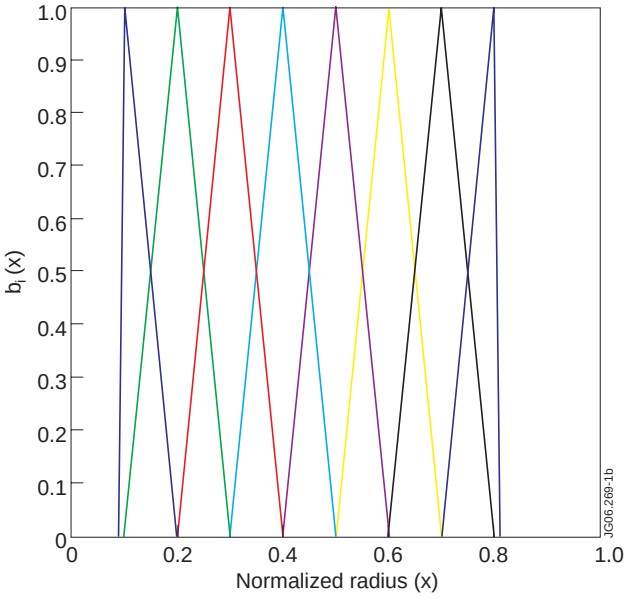

Figure 1b. Piecewise linear functions used for ρ_{Te}.*

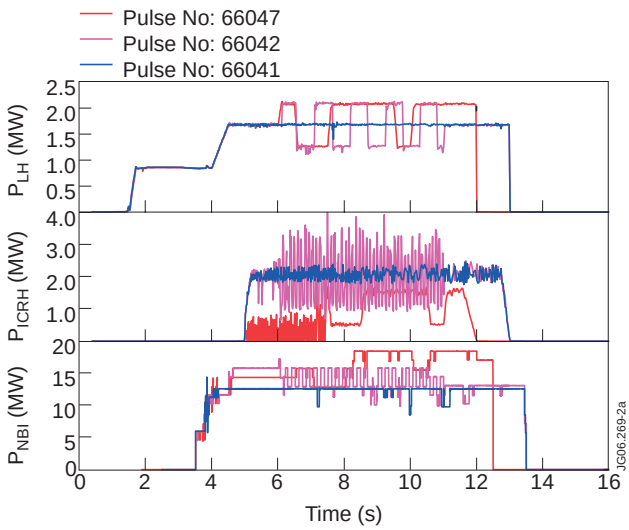

Figure 2. Input LHCD, ICRH and NBI powers for the reference Pulse No: 66041 (blue), and modulated Pulse No's: 66047 (red) and 66042 (magenta).

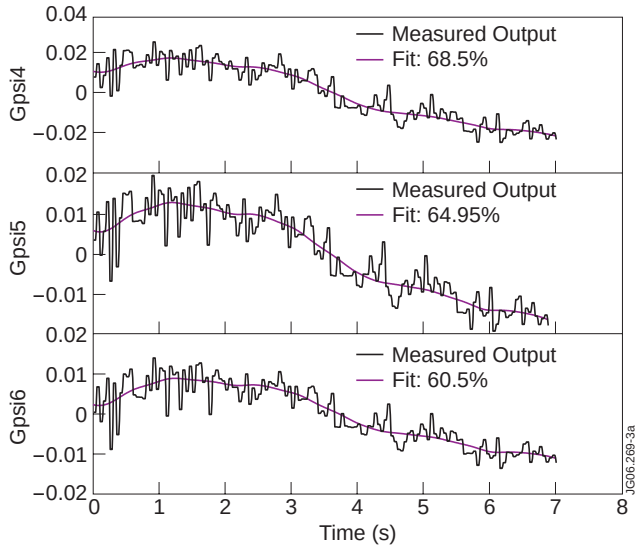

Figure 3. Identification of A_s from the reference pulse data. Comparison between the fit and the experimental data.

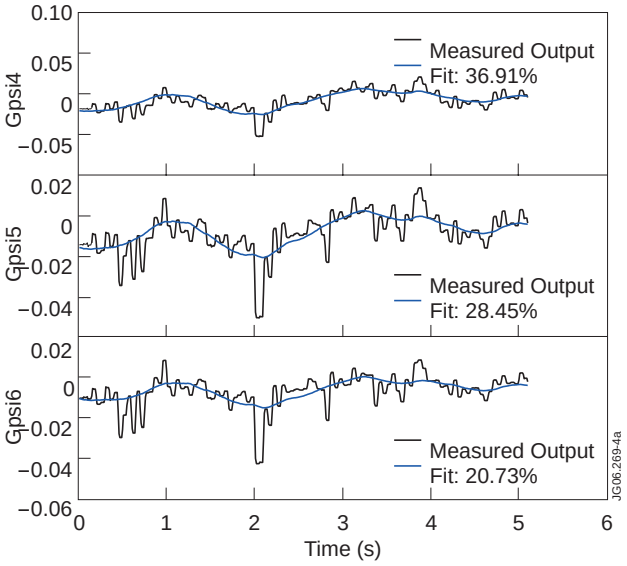

Figure 4. Identification of B_s from Pulse No: 66047. Comparison between the fit and the experimental data.

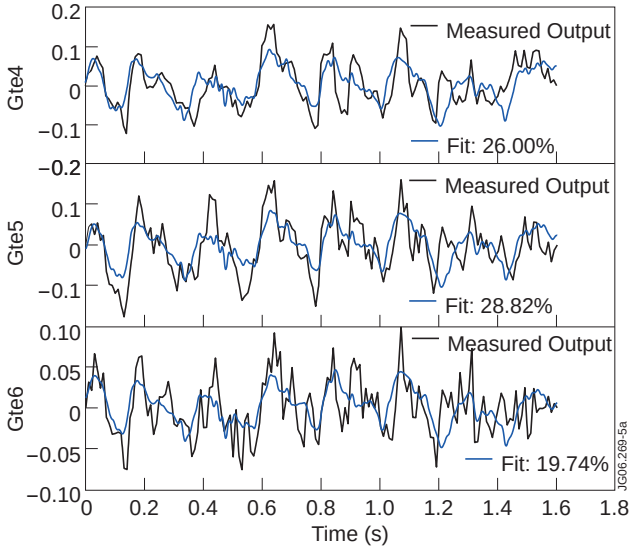

Figure 5: Identification of A_f and B_f from Pulse No: 66042. Comparison between the fit and the experimental data.

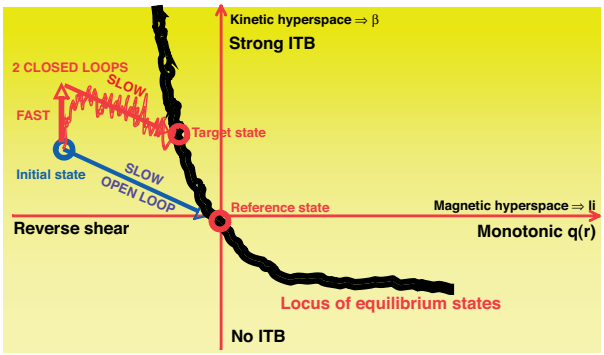

Figure 6: This diagram schematically shows the slow and fast responses of the system to either constant input parameters (blue arrow) or to a change in these parameters (red arrows). Corresponding trajectories are shown in state space. Lines and curves are artistic 1-D representations of multidimensional spaces.

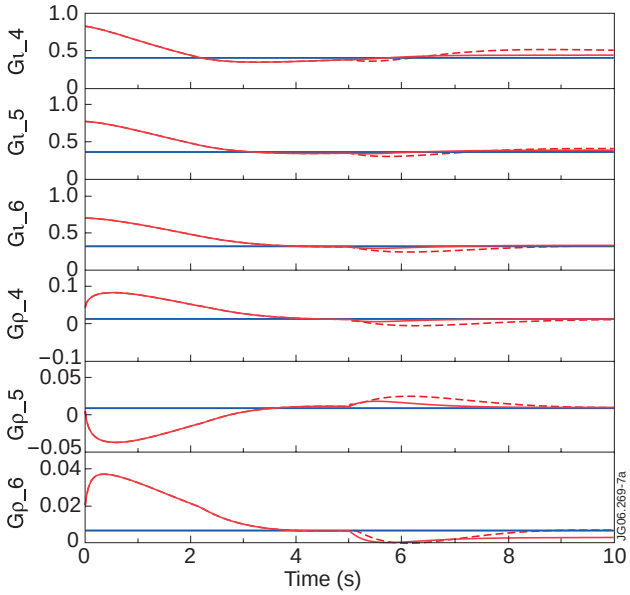

Figure 7: Evolution of $\iota(x)$(upper traces) and $\rho_{Te*}(x)$ (lower traces) at x = 0.4, 0.5 and 0.6 in a closed-loop simulation with (full) and without (dotted) disturbance rejection. The requested target values are shown by the horizontal lines.

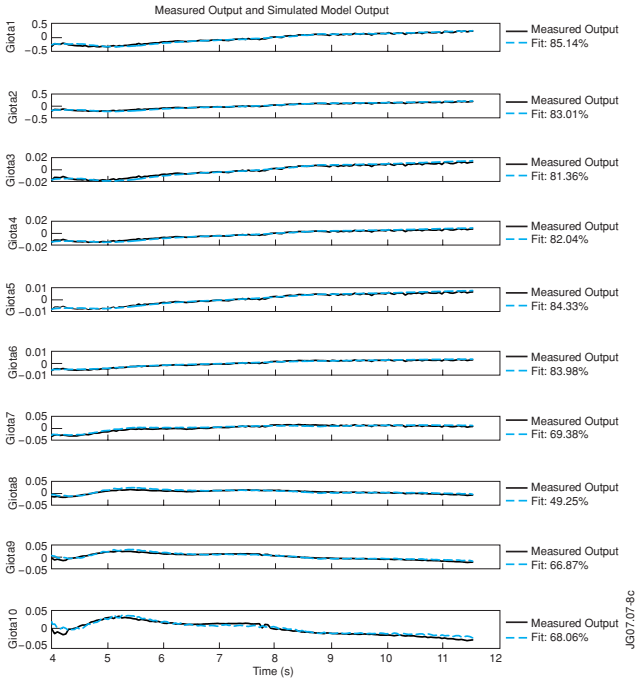

Figure 8: Evolution of the actuator powers in the closed-loop simulation with (full) and without (dotted) disturbance rejection.

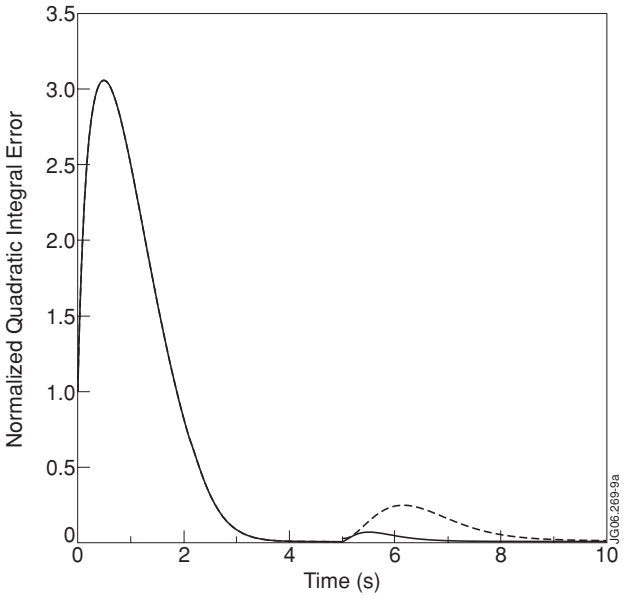

Figure 9: Evolution of the cost functional I in the closed-loop simulation with (full) and without (dotted) disturbance rejection.

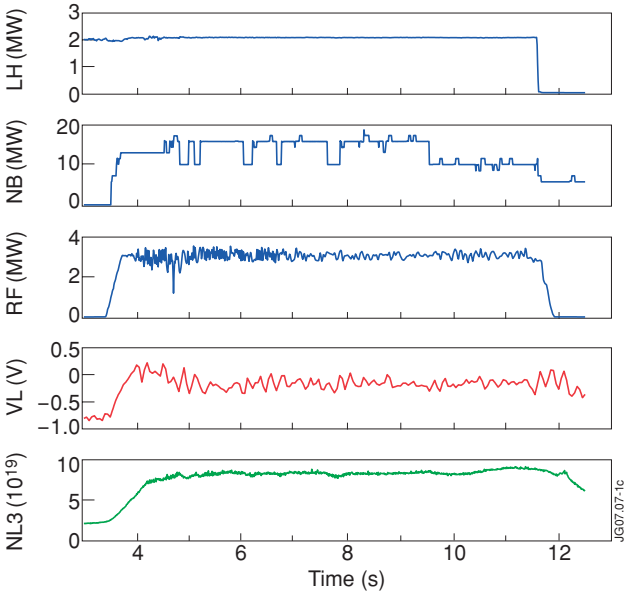

Figure 10: Input powers (blue) for modulated Pulse No: 67874, loop voltage (red) and line integrated density (green).

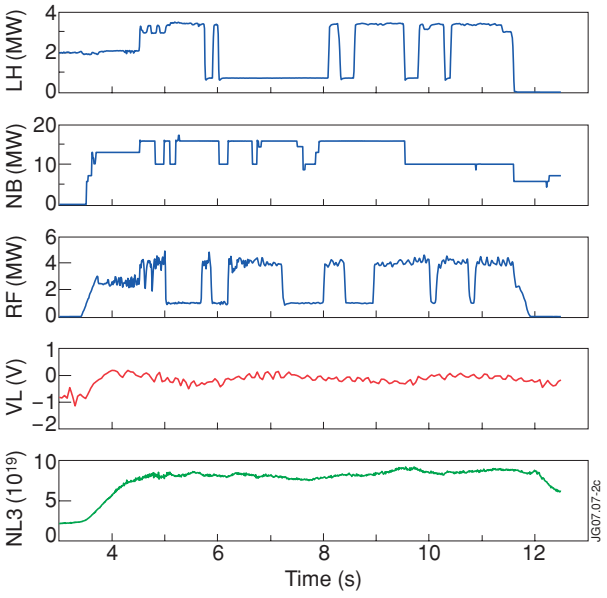

Figure 11: Input powers (blue) for modulated Pulse No: 67876, loop voltage (red) and line integrated density (green).

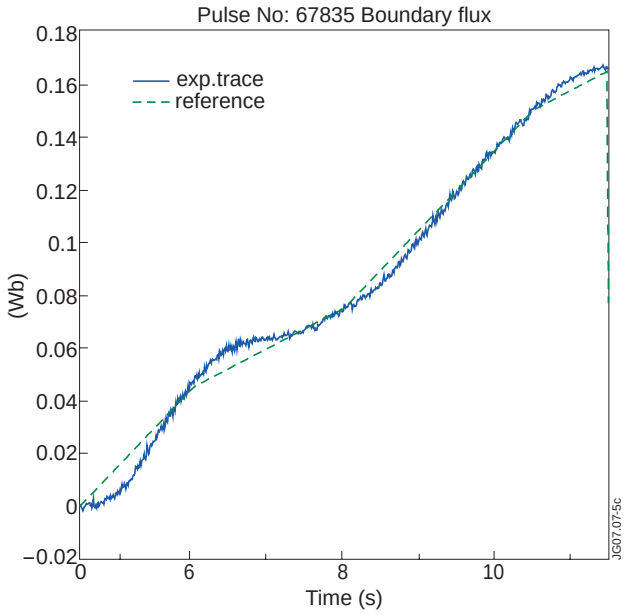

Figure 12a: Control of the boundary flux through the PC, Pulse No: 67835, using the PF system as an actuator.

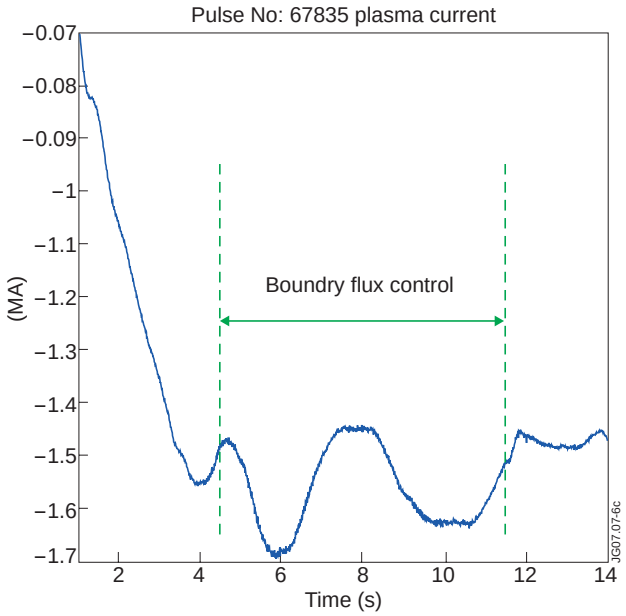

Figure 12b: Time evolution of the plasma current during the control of the boundary flux through he PC, Pulse No: 67835.

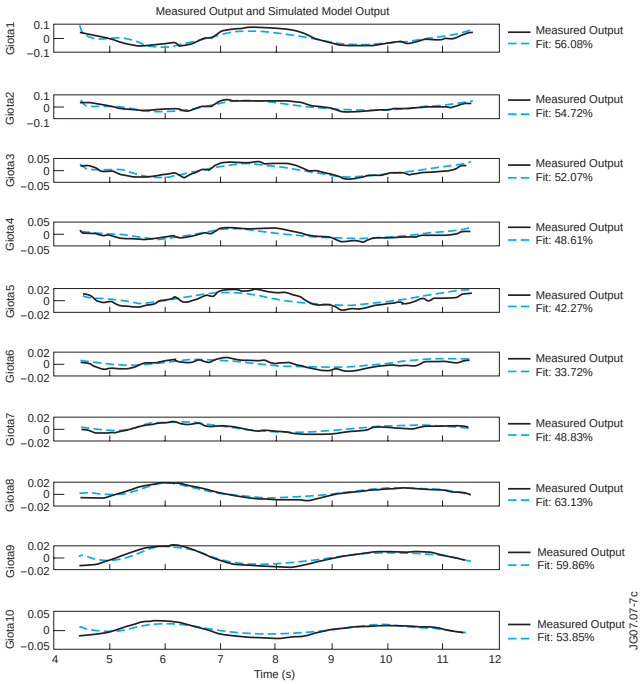

Figure 13: Comparison between reconstructed and measured iota profile, Pulse No: 67840 at 10 fixed normalized radii.

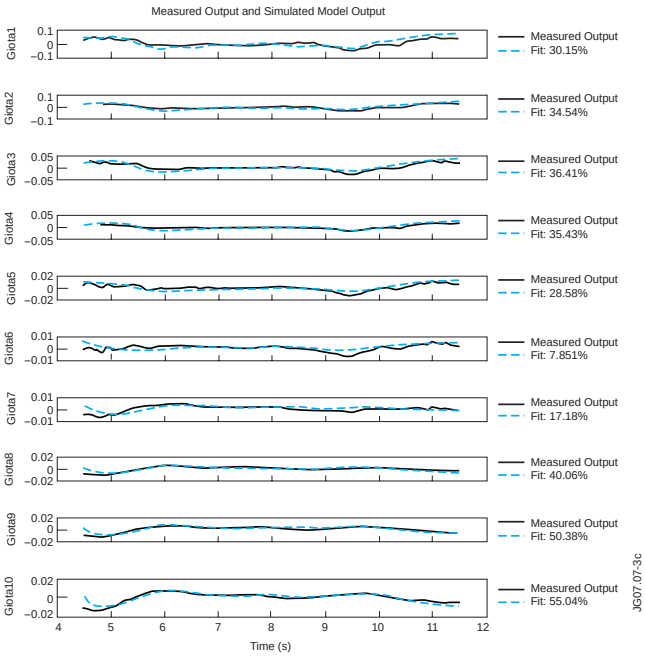

Figure 14: Comparison between reconstructed and measured iota profile, Pulse No: 67874 at 10 fixed normalized radii.

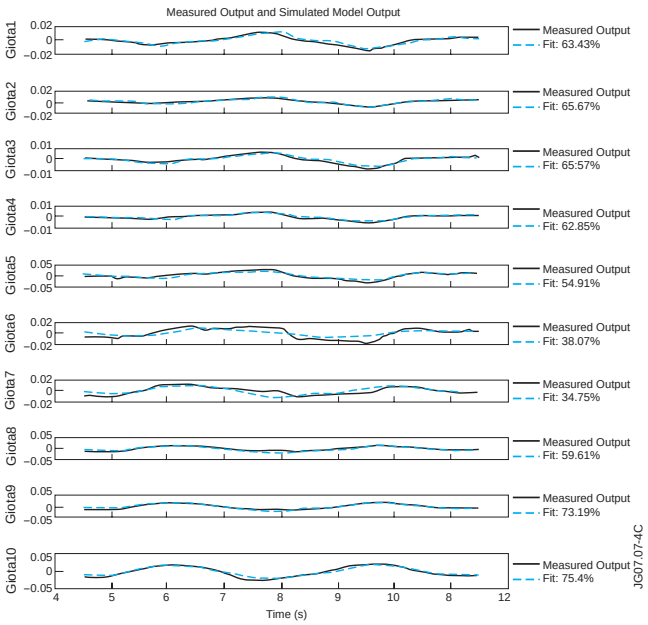

Figure 15: Comparison between reconstructed and measured iota profile, Pulse No: 67876 at 10 fixed normalized radii.

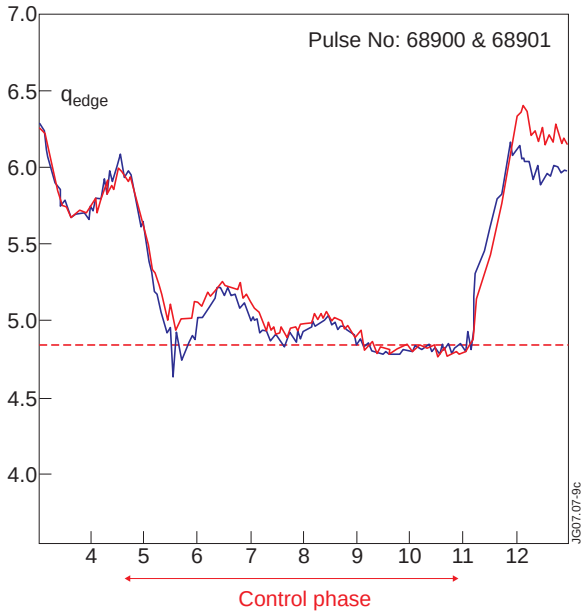

Figure 16: Comparison of qedge control using the PC, using the PF system as an actuator.

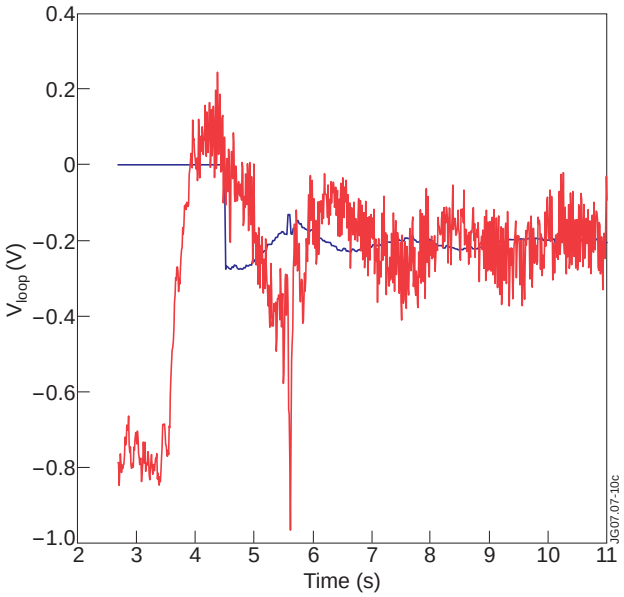

Figure 17: Comparison between requested (blue) and delivered V_{loop} (red) during the control of qedge in Pulse No: 68900.

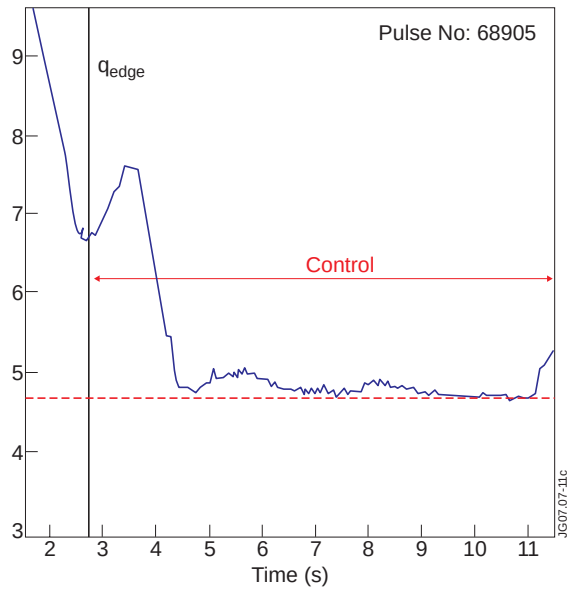

Figure 18: Control of qedge during the current ramp up Pulse No: 68905

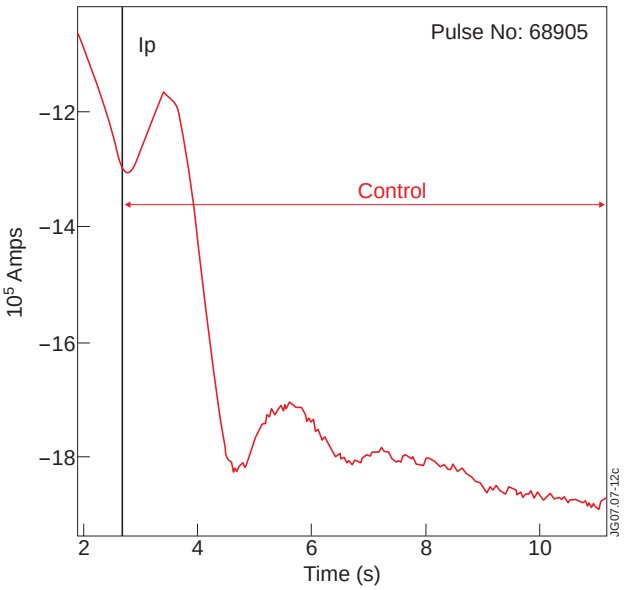

Figure 19: Plasma current evolution during the control of qedge Pulse No: 68905.

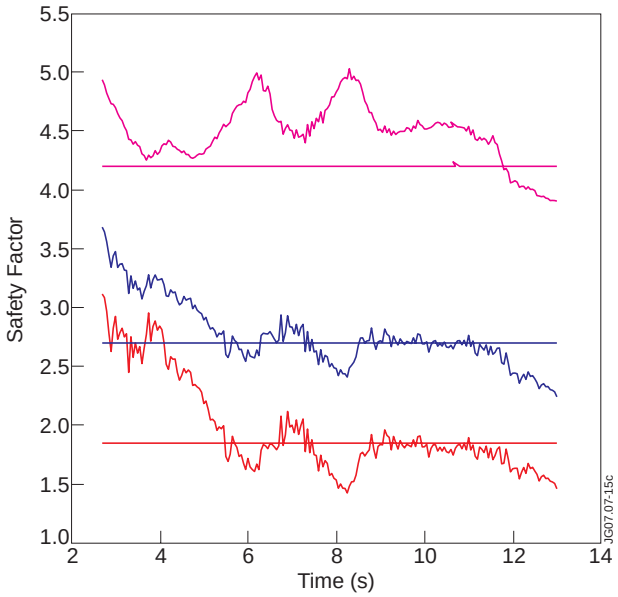

Figure 20: Control of the safety profile at 3 normalised position, x= 0.8 (magenta), x=0.5 (blue), x=0.2 (red) using the 3 H&CD actuators. Pulse No: 70395. During the control phase Vloop is requested constant (32mV/rad).

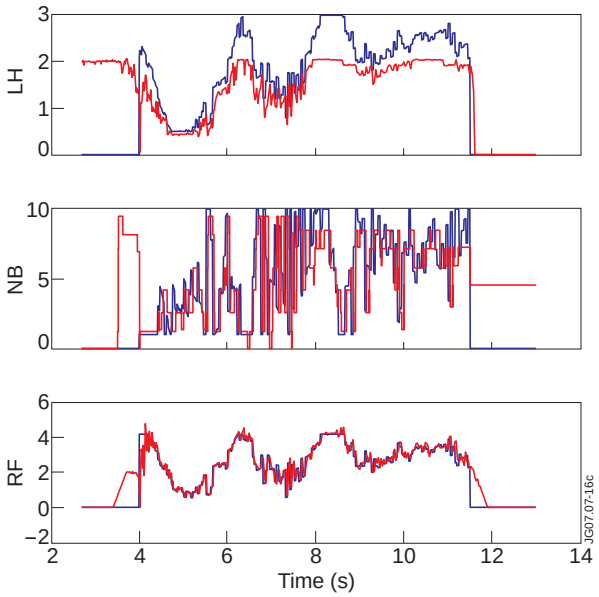

Figure 21: requested and delivered powers for Pulse No: 70395

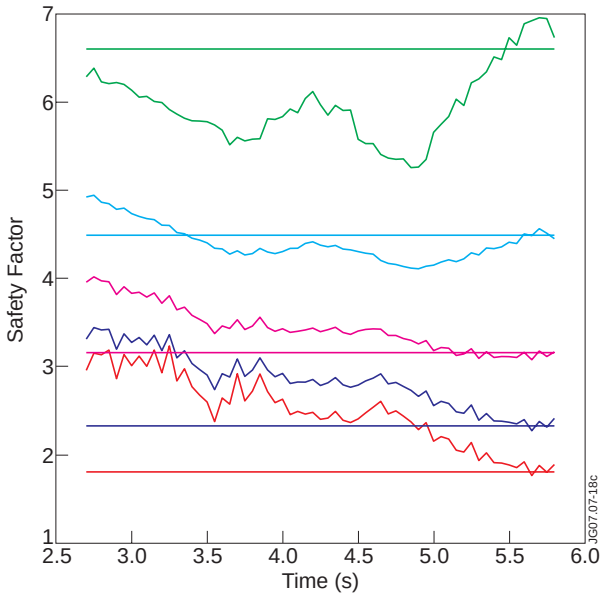

Figure 22: Control of the safety profile at 5 normalised position, x = 1 (green) x = 0.8 (cyan), x = 0.6 (magenta), x = 0.4 (blue), x = 0.2 (red) using the 3 H&CD actuators. Pulse No: 70395.